

# *Numerical Simulation Research on Paste Filling Mining of Metal Mines Based on Blockchain Technology under the Background of Agricultural Environmental Protection*

**Rosa Cantero**\*

*University of Frankfurt, Germany*

*\*corresponding author*

**Keywords:** Blockchain Technology, Paste Filling Mining, Agricultural Environmental Protection, Numerical Simulation Research

**Abstract:** In recent years, environmental protection and sustainable development have become important directions in my country's development strategy. In response to the concept of "green mining", this article focuses on metal mine mining and conducts a numerical simulation study on paste filling technology. Compared with traditional mining methods, the range of materials available for paste filling is wider, which has a more positive impact on environmental protection. This paper combines blockchain technology with numerical simulation research to compare and analyze the filling rate of different filling methods and the damage to the overlying strata during mining, highlighting the technical advantages of paste filling mining. In the laboratory experiment, this article optimizes and adjusts the paste ratio, and studies the influence of materials on the strength of paste by adjusting a single factor. At the same time, this paper analyzes the filling effect of the paste filling body and its control effect on the surface subsidence, and compares the observation data with the actual surface to verify the accuracy of the numerical simulation. From the experimental data, when calculating the surface subsidence coefficient, according to the maximum surface subsidence value and the maximum horizontal movement value obtained by the simulation, the surface subsidence coefficient of the straddle method is calculated to be 0.67, and the surface subsidence coefficient of paste filling mining is 0.02, About 2% of the subsidence coefficient of the subsidence method. It can be seen that paste filling mining has a significant effect in controlling surface subsidence.

## **1. Introduction**

Mining is an important foundation of the country's economy and energy, and it is of great significance to the mining of minerals in human social activities. However, in the process of mining,

it may cause problems such as ground subsidence in the mining area, expansion of the water-conducting fissure zone and flooding, and the mining area will face greater engineering disasters due to roadway and stope instability. After the ore was mined, a huge space was left in the mining area, which caused the initial balance of the earth's crust to become unstable. In the process of recovery from this state, disasters such as loss of stability of the rock mass in the mining area, ground subsidence, and flooding of the fracture zone may occur. These disasters rarely have warning signs when they occur, but the economic losses, social impacts and even casualties caused are huge. Therefore, in the process of mining mines, we must adhere to the principles of sustainable development and agricultural environmental protection, strictly control all links, and choose the most optimized mining method to ensure the safety of the mining process and maximize economic benefits.

The foreign policy on agricultural environmental protection originated earlier, and the research on sustainable mining has also achieved numerous results. Choudhary has conducted research on the effect of paste filling technology on improving the quality of filling materials. Large voids left by mining work are usually backfilled by broken waste rocks in the form of tailings, and hydraulic fillers and paste fillers are two commonly used backfill options. Choudhary pointed out in the study that paste filling has significantly better stability and practicability than hydraulic filling. Although he explained the characteristics of the materials required for mine paste filling, he did not emphasize the advantages of this technology in environmental protection [1]. Khaldoun has conducted pricing studies on mining waste and tailings using paste filling solutions. The storage of mine wastes and process tailings is one of the important challenges facing mining operations. The major part of plant treatment emissions and waste rock development are usually stored in surface areas. The volume and chemical properties of these materials pose serious problems for the required storage space, and paste filling is an ingenious solution to minimize the storage of tailings. From the experimental data, paste filling does have obvious advantages over other filling methods in this respect. If more filling material ratio experiments can be carried out, more experimental results may be obtained [2].

With the development of economy and technology, my country has paid more and more attention to agricultural environmental protection and sustainable development. Scholars have also conducted various studies on green mining. Liu Y and his team conducted chemical experiments on the application of raw powder in mine paste filling. The study uses alkali, calcium, and sulfur as the main materials, and uses the orthogonal test method to analyze the effects of early strength agents, quicklime, and gypsum on the pozzolan activity of recycled powder. Using setting time and early compressive strength as the analysis indicators and carrying out a range analysis, it is found that the best ratio of recycled powder cementitious materials for slurry backfilling is recycled powder: fast lime: gypsum: early strength agent. From the experimental data, the regenerated split body can have a good effect as the gel material in the paste filling, but concrete practice is needed to verify the feasibility of the material ratio [3].

Based on the Internet and computer technology, this paper conducts in-depth research on the establishment of a customized system model for epidemiological survey data collection. The research is mainly carried out from the following aspects: First, this article introduces various technologies and methods used in the sustainable development of mining. These include blockchain technology, paste filling mining technology, blockchain-based searchable encryption algorithms, and blockchain-based data integrity verification models. Next, this paper carried out a numerical simulation experiment of paste filling mining, and briefly explained the material ratio and numerical model of paste filling experiment. Finally, this paper describes in detail the influence of the paste filling raw material ratio on the strength of the paste during the experiment, and predicts the effect of filling technology.

## 2. Numerical Simulation Technology of Mining Based on Blockchain

### 2.1. Blockchain Technology

Blockchain is a decentralized, trustless, and collectively maintained distributed database system. The database is an ordered data block generated using cryptographic algorithms [4]. Blockchain technology uses encryption algorithms, timestamp technology, and consensus mechanisms to enable the nodes participating in the system to realize point-to-point information exchange without trusting each other [5]. The Merkle tree data structure provided by the blockchain and the consensus mechanism based on proof-of-work ensure the immutability and traceability of transactions on the chain [6]. The participating nodes in the permission block chain system are authorized to set up. Some permission chains do not have a digital currency mechanism, and some nodes have been designated in the system to keep accounts without the need to use encrypted currency to encourage nodes to compete for keeping accounts [7]. The nodes on the permission chain are granted specific permissions, so that they can exert effects on specific functions, such as reading and accessing information in the block chain [8].

In the process of paste filling mining in metal mines, adherence to environmental protection and sustainable development has become an important research direction during mining in various regions. As a decentralized database, the blockchain can realize cooperation between multiple subjects through information exchange and sharing. When conducting numerical simulation research, it can also conduct better simulation experiments through the security guarantee system of the blockchain[9-10].

### 2.2. Paste Filling Mining Technology

The principle of rock formation control for paste filling mining is to fill the goaf behind the support during the advancement of the working face. Generally speaking, the entire goaf behind is taken as one through the process of isolation, filling, and solidification. The passive support system basically eliminates the falling space of the roof of the goaf [11]. Compared with traditional filling methods, paste filling can not only increase the overall strength of the filling, but also has a better performance in environmental protection.

At present, some mines in our country have carried out the industrial practice of high-efficiency paste filling, but its theoretical research has not kept up with the pace of production practice, especially in the study of the control of the paste filling face, no paste filling coal face support has been established, The real mining physical process of the interaction between the filling body and the direct roof and the lower basic roof. The current overlying rock movement, surface subsidence law and the control of the working face are very low, so it is difficult to realize the design of the paste filling surface support and filling materials Provide effective scientific basis. On the whole, the control of the rock formation of the paste filling face is the theoretical basis of paste filling mining [12].

The paste-filling mining system is a complex system, which has the characteristics of integrity, relevance, structure, timing, functionality, and openness that a general system has. It is composed of many subsystems and can be used in a large range. The paste filling system is defined as the entire mine production system that adopts the paste filling ore method. In a general sense, the paste filling system can be defined as the material preparation composed of the feeding system, the pipeline feeding system and the filling control system. And transport system [13]. The paste-filling mining process is regarded as an evaluation system. The paste-filling mining system is a subsystem of the entire mine production system. The safety of its operation status is closely related to the operation status and changes of adjacent systems and the entire system [14].

### 2.3. Searchable Encryption Algorithm Based on Blockchain

The research of traditional searchable encryption technology is based on cloud server [15]. Cloud servers provide users with data storage and search services, but cloud servers cannot guarantee the security of stored data. In order to prevent the leakage of related data information, the data owner uploads the encrypted data to the cloud server, and then the cloud server implements the data search function on the ciphertext, and finally the cloud server returns the ciphertext search result related to the search keyword [16].

In symmetric searchable encryption, the encryption and decryption of the ciphertext are done by the holder of the private key. Therefore, the management of private keys is a problem faced by symmetric encryption systems. SSE is mainly applied to the premise that the data user knows the data owner's key or the data user and the data owner are the same person. Unless the data user has the user's private key, the search results cannot be decrypted [17]. Figure 1 is a system model diagram of symmetric searchable encryption.

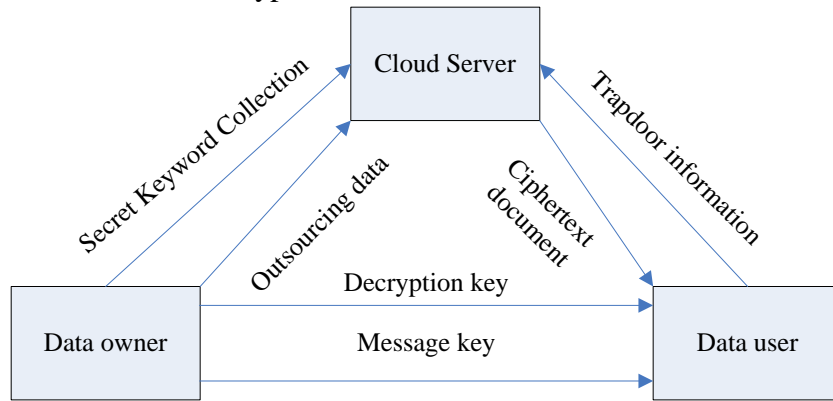


Figure 1. Symmetric searchable encryption system model

An attribute searchable encryption scheme is proposed using attribute encryption algorithm. In the attribute searchable solution, the data is encrypted using an access structure with attribute characteristics, and then the cloud server searches for information that contains the keyword and meets the access structure according to the threshold value generated by the user [18-19]. The blockchain-based searchable encryption algorithm security model scheme is as follows.

Enter the safety parameter  $\lambda$ , select  $G_1$  and  $G_2$  as the  $P$ -order cyclic group. The system randomly selects  $\alpha, \beta \in \mathbb{Z}_p$  and keeps  $msk$  secret, then the master key satisfies the formula:

$$msk = (\alpha, \beta) \quad (1)$$

The system administrator randomly selects  $r \in \mathbb{Z}_p$ , and the attribute authority center sends the key to the user, then the key  $sk$  satisfies the formula:

$$sk = (R, R', \{X_a, Y_a\}_{\forall a \in S}) \quad (2)$$

After constructing a polynomial equation about the keyword  $W$ , the formula can be obtained:

$$g(x) = a(x - H_1(w_1))(x - H_1(w_2)) \wedge (x - H_1(w_m)) + b \quad (3)$$

$$g(x) = a_m x^m + a_{m-1} x^{m-1} + \wedge a_1 x + a_0 \quad (4)$$

The keyword index  $I$  is stored on a separate keyword set server, and then broadcasted by the transaction TX of the server, and finally stored on the permission blockchain [20]. The index  $I$  and the authorized ciphertext formula satisfy:

$$I = (L_j, F_0, F_1, \{(A_v, B_v) | v \in \Gamma\}) \quad (5)$$

$$C_M = (\Gamma, C_0, C_1) \quad (6)$$

Randomly select  $t^a \in Z_p$  for each attribute, D sends  $(\eta_1, \eta_2, h')$  to the server, and the server verifies equation (7) after calculation.

$$H_3(h^*) = \mu \quad (7)$$

The verification process is as follows:

$$H_3(h^*) = H_3 \left( H_2 \left( \frac{\eta_1}{\eta_2^{H_1(a)}} \right) \oplus h' \right) \quad (8)$$

$$H_3(h^*) = H_3 \left( H_2 \left( \frac{g_1^{r_1 r_2} g_1^{r_2 t^a H_1(a)}}{g_1^{r_2 t^a H_1(a)}} \right) \oplus h' \right) \quad (9)$$

$$H_3(h^*) = H_3(H_2(g_1^{r_1 r_2}) \oplus h') = H_3(h) \quad (10)$$

The data user constructs a trapdoor corresponding to the key set W, and randomly selects  $r_3 = Z_p^*$ . The trapdoor of the keyword set is  $T_{W'}$ , and its expression is:

$$T_{W'} = (K_0, K_1, E_i, \{(X_a, Y_a) | a \in S\}) \quad (11)$$

The searcher on the permission chain calculates the secret value E of the leaf node according to the attribute in the trapdoor. If the attribute satisfies the access number structure, the searcher needs to judge whether the equation (12) is equal [21].

$$e(F_0, K_0) = E_v \cdot e(F_1, K_1) \prod_{i,j=0}^m e(L_i, K_i) \quad (12)$$

If they are equal, the searcher will broadcast the correct search results in the form of transactions. The correctness verification process is as follows:

$$e(F_0, K_0) = e(g_2^h, g_2^b, g_1^{ar_3}) = e(g_1, g_2)^{har_3+bar_3} \quad (13)$$

$$E_v \cdot e(F_1, K_1) = e(g_1, g_2)^{har_3} \quad (14)$$

$$\prod_{i,j=0}^m e(L_i, K_i) = e(g_1, g_2)^{ar_3b} \quad (15)$$

## 2.4. Blockchain-Based Data Integrity Verification Model

Provable safety theory is essentially to prove the feasibility of various safety schemes. Generally speaking, this research method can be divided into two categories, namely, computational complexity security and information theory security [22]. Among them, information theory security is an unconditional security, so it has very high requirements for security standards, and it is difficult to achieve it in all solutions. Therefore, the blockchain-based data integrity verification model in this article belongs to computational complexity security.

The most commonly used signature mechanisms at this stage include DSA signatures and RSA signatures. Compared with these signature mechanisms, the BLS (Boneh-Lynn-Shacham) signature

mechanism has certain advantages in the length of the signature digits [23]. In addition, BLS signatures spend less on communication and storage costs. Combined with the particularity of bilinear distribution encryption in elliptic curve encryption, the data integrity can be proved under the random oracle model [24].

The security analysis of the model is as follows: Under the premise that CSP is the adversary and TPA is the emulator, control the random prediction  $H$ , set  $v = g^\omega, u = g^a h^b, a, b \leftarrow Z_p$  to be the random value selected by the emulator, and then execute the random prediction model:

$$H(i) = g^{r_i} / (g^{a m_i} \cdot h^{b m_i}) \quad (16)$$

At that time  $u = g^a h^b$ , the simulation can calculate the signature set:

$$H(i) \cdot u^{m_i} = g^{r_i} \quad (17)$$

$$\sigma_i = (H(i) \cdot u^{m_i})^\omega = (g^\omega)^{r_i} \quad (18)$$

The honest CSP will return  $P = (\mu, \sigma, R)$  to TPA and satisfy the equation:

$$e(\sigma, g) = e\left(\prod_{i=S1}^{S_c} h(i)^{v_i} \cdot u^\mu \cdot R^{-h(R)}, v\right) \quad (19)$$

When  $r$  is the same for all verification equations, then:

$$e\left(\frac{\sigma'}{\sigma}, g\right) = w(u^{\Delta\mu}, v) \quad (20)$$

Dynamic measurement is a very important step when performing audit tasks. The key point is the way to collect credible evidence. In addition, the credibility verification of the task is also the key to the research [25]. According to the verification method studied in this paper, the integrity measurement of the model can be effectively achieved.

### 3. Numerical Simulation Experiment of Paste Filling Mining Based on Blockchain

#### 3.1. Experimental Background

The surface subsidence is caused by the movement and destruction of the overburden. Therefore, controlling the movement and destruction of the overlying rock is also controlling the surface subsidence. For paste cemented filling mining, the surface will also sink. However, since the goaf is filled immediately after mining and a filling body with a certain strength is formed, the filling body has a certain restrictive effect on the movement of the overburden, and controls the movement and destruction of the overburden to a certain extent[26-27]. Therefore, in order to study the destruction process and scope of the overlying strata in mining, this article will use numerical simulation research methods to conduct quantitative research and analysis. In this paper, FLAC3D numerical simulation software is selected to establish a numerical simulation model to study the numerical simulation scheme of the change law of the deformation and failure of the overburden under different filling rates.

#### 3.2. Paste Filling Experiment Material Ratio

The prerequisite for paste production is to select suitable materials, and its performance indicators play a key role in controlling the strength of the paste after filling. There are currently

many paste filling materials. Refer to the successful experience of paste filling technology in the area in recent years. The materials selected for the study mainly include aeolian sand, loess, fly ash, and cement from local cement plants with extensive ground coverage.

The aeolian sand in this experimental area is silt, which has low viscosity content. The content of gravel is mainly silt fine sand. The silty sand has uniform particles, poor gradation, low surface activity, no viscosity, and obvious non-plasticity. From the perspective of building materials, the natural gradation of its particle size is poor, and it is not recommended to be used as building concrete and mortar. However, from the perspective of paste filling, the strength of the paste to be prepared is low, so it is used as a filling material. Aggregate is realistic and maneuverable.

The fly ash was taken from the thermal power plant on the northeast side of the study area. Fly ash can improve the workability, impermeability, air permeability, sulfate resistance and chemical corrosion resistance of the paste slurry, and improve the workability of the slurry. Improve the high temperature resistance of concrete, reduce particle separation and water separation, and reduce shrinkage and cracking of concrete[28-29].

The loess was taken from the southern surface of the mining area. The main minerals of loess are feldspar, quartz, mica, silicate, illite, and montmorillonite. The main chemical composition of loess is similar to that of aeolian sand, its plasticity is good, and the particle gradation is good. Due to the poor gradation of aeolian sand aggregate, loess is introduced to compensate for the gap between aeolian sand and increase the friction between particles. Strength and adhesion, thereby increasing the late strength of the prepared paste.

After the cement meets with water, various gels and crystals are formed through hydration reaction, so that the loose cement powder particles become cement paste. Adding gravel, fly ash, loess, etc. to the cement to participate in the hydration reaction can effectively eliminate the negative factors caused by calcium hydroxide, thereby enhancing the strength of the mixture.

### 3.3. Numerical Model of Paste Filling Mining

FLAC3D is a three-dimensional finite difference program. This article will use it to simulate and analyze the plastic flow of the three-dimensional structure of soil, rock and other materials. During the mining process, the overlying rock movement law, the experimental simulation conditions used the actual geological conditions of the mine under the same geological conditions, the filling rate is respectively: 50%, 75% and 90% experimental models, used to simulate the stope during the filling mining process the law of overburden movement. Table 1 shows the mechanical performance parameters of the rock formation.

*Table 1. Mechanical properties of rock formations*

Rock formation	Bulk density	Compression/MPa	Cohesion/M Pa
Sandstone layer	2.56	60.0	16.0
Mudstone	2.23	27.0	6.0
Interbedded mudstone and sandstone	2.31	432	7.8
Interbedded mudstone and sandstone	2.46	191	10.5
Shale	2.33	75.8	6.2

The average inclination of the ore body in this simulation is 30°, the average buried depth is

about 128m, and the height of the ore body is about 77m. The overlying strata of the ore body are about 31m in the Lower Cretaceous Dongjing Formation, and about 31m in the Upper Permian Douling Formation. 80m, about 21m of the Dangchong Formation of the Lower Permian System and about 30m of the Lower Permian Qixia Formation of the underlying surrounding rock. The key to the success of filling mining lies in the control of the overlying strata and the surface.

#### 4. Numerical Simulation of Paste Filling Mining in Metal Mines Based on Blockchain

##### 4.1. Experimental Analysis of Raw Material Ratio of Paste Filling

According to the theoretical requirements of paste strength, this article will select reasonable filling materials according to local conditions according to the geographical situation of the study area, and optimize and adjust the paste ratio through indoor experiments, and study the influence of materials on the strength of paste by adjusting a single factor law. Table 2 and Figure 2 show the results of laser particle size analysis of aeolian sand.

Table 2. Aeolian sand laser particle size analysis

Particle diameter	Percentage%	Accumulation%	Particle diameter	Percentage%	Accumulation%
0.214-0.272	0.04	0.05	1.153-1.481	0.03	1.51
0.272-0.346	0.21	0.26	1.481-1.888	0.02	1.53
0.346-0.442	0.32	0.58	1.888-2.401	0.05	1.58
0.442-0.563	0.25	0.83	2.401-3.055	0.15	1.73
0.563-0.717	0.26	1.09	3.055-3.872	0.23	1.96
0.717-0.912	0.23	1.32	3.872-4.953	0.32	2.28
0.912-1.153	0.16	4.48	4.953-6.628	0.41	2.69

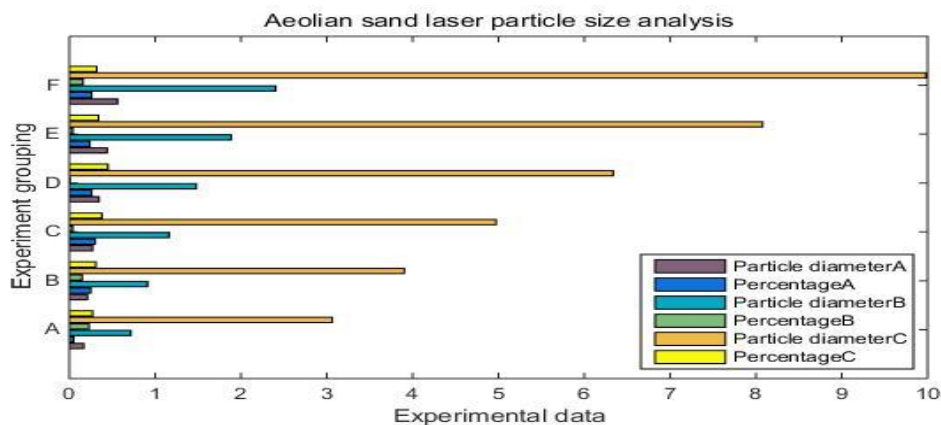


Figure 2. Aeolian sand laser particle size analysis

It can be seen from Table 2 and Figure 2 that the main components of aeolian sand are SiO<sub>2</sub>, Al<sub>2</sub>O<sub>3</sub>, CaO, MgO and Fe<sub>2</sub>O<sub>3</sub>, among which SiO<sub>2</sub> and Al<sub>2</sub>O<sub>3</sub> account for about 80%, with an average density of 1.63g/cm<sup>3</sup> and a porosity of about 40.3 %; In the experiment, according to the laser particle size analyzer, the specific surface area is 986cm<sup>2</sup>/g, the particle size distribution is between 0.168~483.2μm, and the particles between 0.076~0.27mm account for 72.43% of the total mass, which is 0.27m~ Particles between 0.51mm accounted for 4.42% of the total mass, and particles smaller than 0.076mm accounted for 23.15% of the total mass.

According to ASTM standards, raw materials with calcium oxide content greater than 10% belong to class C fly ash, which is mainly formed after burning lignite and sub-bituminous coal. Its chemical composition is similar to cement. It is often used to replace part of cement to reduce production costs. Table 3 and Figure 3 are the results of fly ash laser particle size analysis.

Table 3. Fly ash laser particle size analysis

Particle diameter	Percentag e%	Accumulatio n%	Particle diameter	Percentag e%	Accumulatio n%
0.062-0.081	0.06	0.06	0.552-0.736	1.21	7.81
0.081-0.103	0.35	0.41	0.736-0.926	1.35	9.16
0.103-0.168	0.62	1.03	0.926-1.163	1.48	10.64
0.168-0.232	0.97	2	1.163-1.521	1.63	12.27
0.232-0.278	1.23	3.23	1.521-1.883	0.85	13.12
0.278-0.356	1.55	4.78	1.883-2.305	0.53	13.65
0.356-0.512	1.82	6.6	2.305-3.176	1.82	15.47

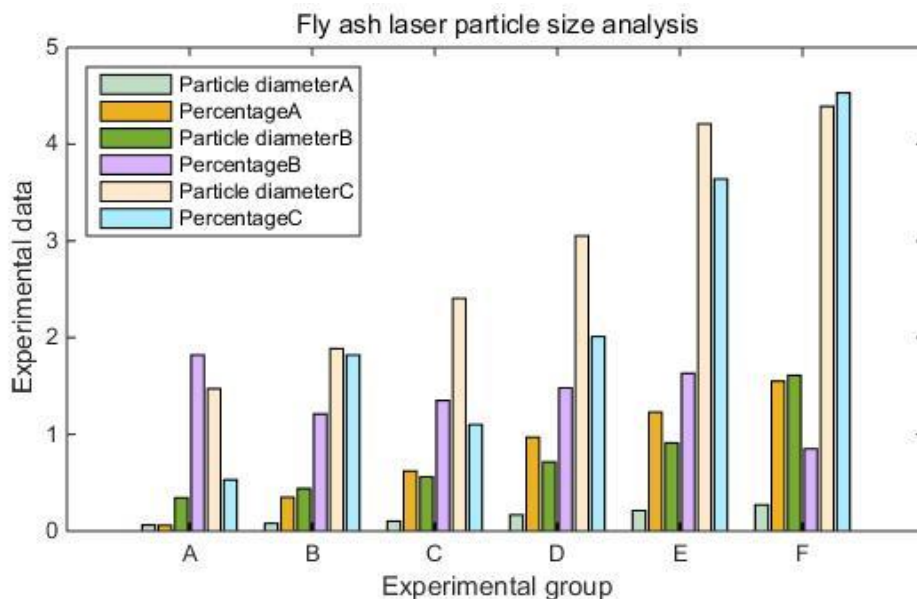


Figure 3. Fly ash laser particle size analysis

It can be seen from Table 3 and Figure 3 that the main components of fly ash are SiO<sub>2</sub>, Al<sub>2</sub>O<sub>3</sub>, Fe<sub>2</sub>O<sub>3</sub>, CaO, and insufficiently burned charcoal, etc. It also contains a small amount of K, P, S, Mg and other compounds and As, Cu, Zn, etc. Trace elements. The measured average dry density of fly ash is 1.22g/cm<sup>3</sup>. According to the analysis of the laser particle size analyzer, the specific surface area is 9788cm<sup>2</sup>/g, the particle diameter is between 0.06~183.2μm, and 96.07% of the particles are less than 0.1mm in diameter. The particles are mostly powdery. Table 4 and Figure 4 show the results of laser particle size analysis of loess.

Table 4. laser particle size analysis of loess

Particle diameter	Percentage	Accumulation	Particle diameter	Percentage	Accumulation
	e%	n%		e%	n%
0.082-0.105	0.05	0.05	0.561-0.722	1.03	5.29
0.105-0.133	0.31	0.36	0.722-0.895	0.88	6.17
0.133-0.168	0.29	0.65	0.895-1.053	0.65	6.82
0.168-0.221	0.58	1.23	1.053-1.352	0.36	7.18
0.221-0.353	0.86	2.09	1.352-1.621	0.21	7.39
0.353-0.442	1.05	3.14	1.621-1.958	0.36	7.75
0.442-0.561	1.12	4.26	1.958-2.425	1.42	9.17

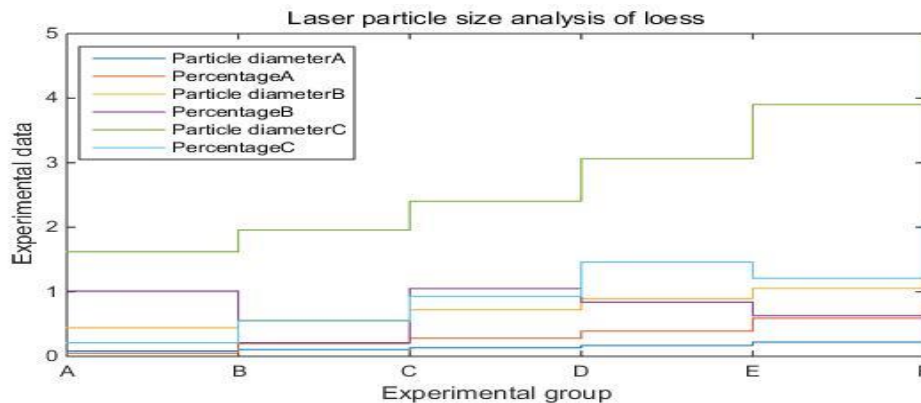


Figure 4. Laser particle size analysis of loess

It can be seen from Table 4 and Figure 4 that the main components of loess in this experiment are SiO<sub>2</sub>, Al<sub>2</sub>O<sub>3</sub>, Fe<sub>2</sub>O<sub>3</sub>, CaO, MgO, K<sub>2</sub>O, FeO, etc., and its average density is 1.42g/cm<sup>3</sup>. In the experiment, the specific surface area was analyzed by the laser particle size analyzer. 4068cm<sup>2</sup>/g, the particle diameter is between 0.082~388.2μm, and 80% of the particles are less than 0.1mm in diameter.

#### 4.2. Numerical Simulation Analysis of Paste Filling Mining Process

Based on the current mainstream aeolian sand paste filling method, add loess materials, and

study the influence of the content of each material on the strength of the paste, and select the most economical and most suitable strength ratio for the study area. The prepared paste, under the premise of satisfying pumping, must have a later strength of 5.42MPa or more; in order to have better fluidity, its slump should be greater than 200mm.

According to the 1:4:2:1 ratio of cement, aeolian sand, fly ash, and loess, four groups of pastes with mass concentrations of 75%, 76%, 80% and 81% are produced. After the drop test, each group will make 6 copies each, put them into a square mold, cover them with plastic film, and place them in a constant temperature (20°C) and humidity (95%) standard curing box for curing, according to the curing period 3d, 8d, 26d, and 60d respectively measure the compressive strength of two test blocks in each group, and take the average value. The experimental process and results are shown in Table 5, Figure 5 and Figure 6.

Table 5. Basic ratio experiment

Experiment number	Mass ratio				concentration	Slump (mm)	Uniaxial compressive strength/MPa			
	Cement	Aeolian sand	Fly ash	Loess			3d	8d	26d	60d
S1	10	40	20	10	75%	252	0.89	1.27	2.8	4.2
S2					76%	222	1.01	1.33	3.15	5.5
S3					80%	166	1.26	2.02	4.05	6.2
S4					81%	108	1.73	2.55	4.81	7.22

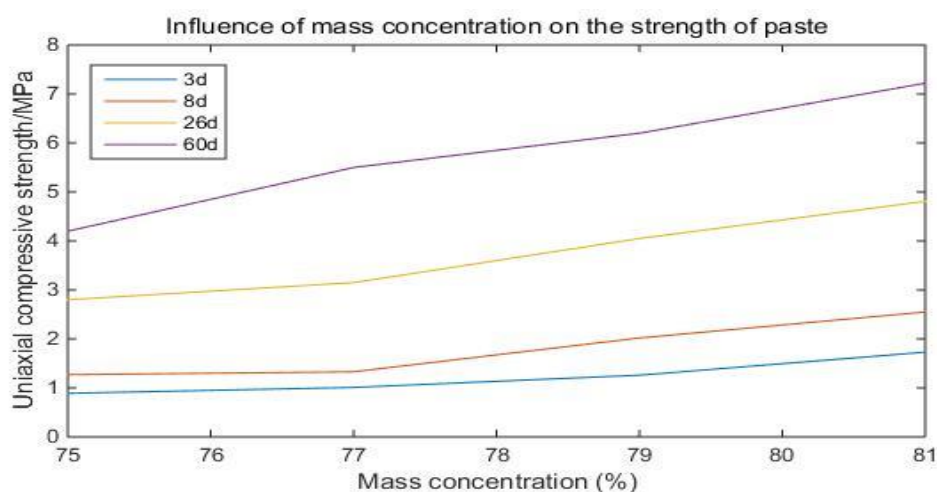


Figure 5. Influence of mass concentration on the strength of paste

It can be seen from Figure 5 and Figure 6 that as the mass concentration increases, the compressive strength of the paste also increases, and the slump of the paste slurry gradually decreases; with the increase of age, the compressive strength of the paste The intensity gradually increases, but the increasing frequency gradually decreases, and finally approaches a certain fixed

value. According to the requirements of the experiment purpose, the slump of the paste in this experiment must be  $> 200\text{mm}$ , and the later strength  $> 5.44\text{ MPa}$ . According to basic experiments, the slump of the two groups of S1 and S2 are up to the standard but the compressive strength of S1 is not up to the standard, S3 and S4 The compressive strength of the two groups of experiments is up to the standard, but the slump is not up to the standard; through the above analysis, it can be seen that the number S2 group meets the purpose of this experiment and can be used as a basic ratio test.

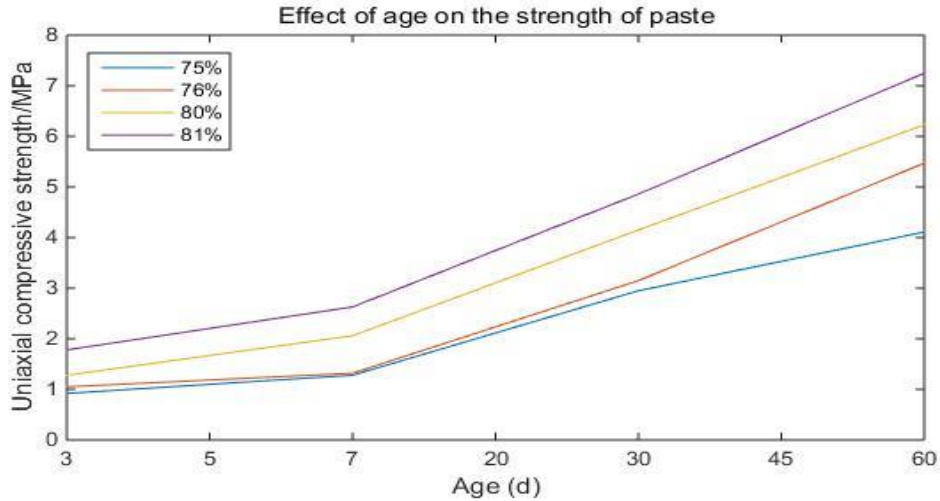


Figure 6. Effect of age on the strength of paste

Based on the geological mining conditions of the working face filling area, a numerical model is established. Take the ground surface as the upper boundary of the model, and the height of the model is 720m. Mining 160m in the oblique direction, in order to eliminate the influence of the boundary, double the average mining depth on both sides; 520m in the strike direction, and 320m on both sides of the strike. The model size is 1120mX1200mX720m. Table 6 shows the maximum surface movement and deformation values when simulating different mining methods.

Table 6. Maximum surface movement deformation value

Mining method	Thickn ess m/mm	sink	Move horizontally	Sink factor	Horizontal movement factor
Paste filling	1700	25	4.2	0.02	0.19
Sinking method	1700	1142	412	0.66	0.35

According to the numerical simulation of mining and filling process in Table 6, it can be seen that the maximum surface subsidence value is 1142mm and the maximum horizontal movement value in the strike direction is 412mm under the conditions of subsidence mining; the maximum surface subsidence value under the paste-filled mining piece is 25mm, and the strike direction The maximum horizontal movement in the direction is 4.2mm. In order to visually see the difference in surface movement and deformation values between nucleus filling mining and subsidence mining, and highlight the advantages of paste filling, this paper will simulate the surface subsidence value and simulated horizontal movement value of paste filling mining and subsidence mining Draw into a curve, as shown in Figure 7 and Figure 8.

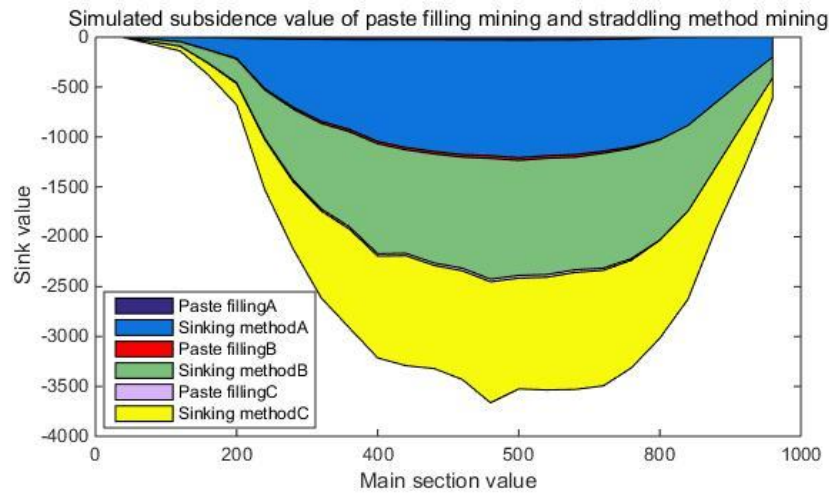


Figure 7. Simulated subsidence value of paste filling mining and straddling method mining

It can be seen from Figures 7 and 8 that the surface subsidence trend and horizontal deformation trend of paste filling mining and subsidence mining are the same. The maximum surface subsidence on the main section of the strike direction of both appears at the center of the goaf, that is, the distance At a horizontal distance of 600m from the model boundary, the horizontal movement value of both of them here is zero. Moreover, the surface subsidence value and horizontal movement value of paste filling mining are far less than that of subsidence mining. It can be seen that paste filling mining can effectively control surface subsidence and protect surface structures.

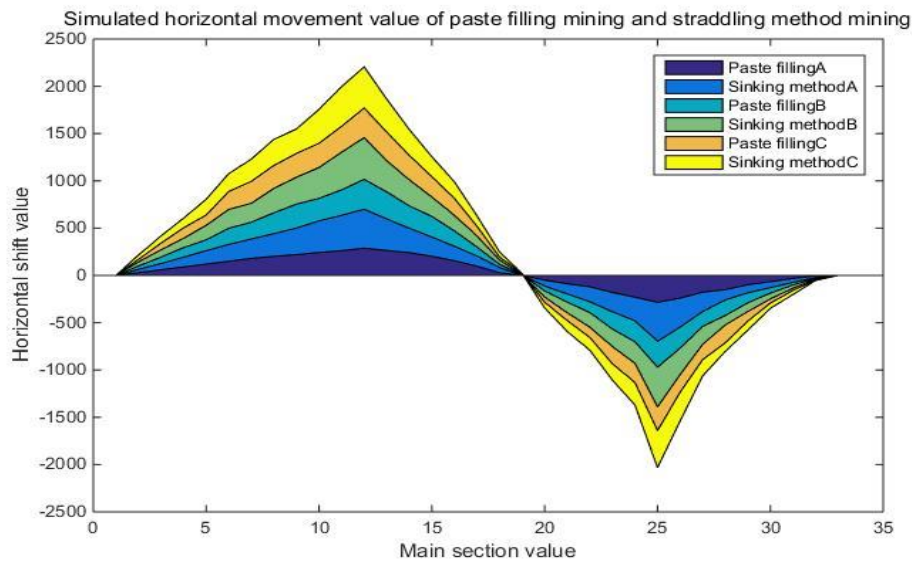


Figure 8. Simulated horizontal movement value of mining

When calculating the surface subsidence coefficient, according to the maximum surface subsidence value and the maximum horizontal movement value obtained by the simulation, the surface subsidence coefficient of the straddle method is calculated to be 0.67, and the surface subsidence coefficient of the paste filling mining is 0.02, which is approximately the subsidence method 2% of the sink factor. It can be seen that paste filling mining has a significant effect on controlling surface subsidence.

## 5. Conclusion

This chapter combines blockchain technology, according to the requirements of paste strength, selects reasonable filling materials according to local conditions, and optimizes and adjusts the ratio of paste through indoor experiments according to the geographical overview of the research area. The influence of body strength. The materials selected in this study are aeolian sand and loess that are widely covered on the surface of the study area. The fly ash and cement are selected as the surrounding power plants and cement plants in the study area. The materials are selected on-site, economical and reasonable, and simple to prepare. The purpose of this experimental study is to find the optimal ratio, the later strength must be more than 5.44MPa, and the slump must be greater than 200mm. While keeping the content of cement, fly ash, aeolian sand and loess unchanged, the strength of the paste increases with the increase in mass concentration, and the fluidity decreases with the increase in mass concentration. Under the condition of keeping the three factors of cement, fly ash and loess unchanged, the single factor of aeolian sand was changed. The experiment found that when the mass concentration is fixed, the slump of the paste slurry before the initial setting varies with the aeolian the sand content increases with the increase, and all meet the requirements of the experimental purpose. The compressive strength decreases with the increase of the aeolian sand content.

This paper analyzes the filling effect of the paste filling body and its control effect on the surface subsidence, and compares the observation data with the actual surface to verify the correctness of the numerical simulation. The key to the success of filling mining lies in the control of the overlying strata and the surface. Therefore, we can start with the causes of overburden failure, study the overburden failure characteristics of caving mining and backfill mining, and study the self-stabilization strength of backfill and the factors affecting surface subsidence controlled by backfill mining. The maximum surface subsidence value under the sinking method is 1142mm, and the maximum horizontal movement value in the strike direction is 412mm; the maximum surface subsidence value under the paste-filled mining material is 25mm, and the maximum horizontal movement value in the strike direction is 4.2mm. It can be seen that paste filling mining has a significant effect on controlling surface subsidence.

In this paper, combining the blockchain technology and the filling mining research technology, through the theoretical analysis of the working face system, the appropriate filling paste aggregate and paste performance parameters are determined, and the indoor paste preparation experiment is carried out according to the theoretical calculation results, Choose a reasonable paste ratio and residue and use simulation software to simulate the entire process of "mining", "filling" and "recycling", and finally proves the advantages of paste filling in mining. In future research, this article believes that the experimental design can be improved from multiple perspectives and more in-depth research can be conducted. For example, adding more ratios of mass concentration, detailed discussion of the basic ratio, and improvement of blockchain-based numerical simulation technology and integrity verification models can also effectively improve the accuracy of research data.

## Funding

This article is not supported by any foundation.

## Data Availability

Data sharing is not applicable to this article as no new data were created or analysed in this study.

## Conflict of Interest

The author states that this article has no conflict of interest.

## References

- [1] B, S, Choudhary. Paste filling - an overview to improve the quality of filling material. *Journal of Mines, Metals & Fuels*, 2015, 63(8):205-213.
- [2] Khaldoun, Abdelhadi, ouadif, et al. Valorization of mining waste and tails through paste filling solution, imager operation, Morocco . *Journal of mining science and technology: English edition*, 2016 (3): 511-516 <https://doi.org/10.1016/j.ijmst.2016.02.021>
- [3] Liu Y , Lu C , Zhang H , et al. Experimental study on chemical activation of recycled powder as a cementitious material in mine paste backfilling. *Environmental Engineering Research*, 2016, 21(4):341-349. <https://doi.org/10.4491/eer.2015.129>
- [4] Lemieux V L . Trusting records: is Blockchain technology the answer?. *Records Management Journal*, 2016, 26(2):110-139. <https://doi.org/10.1108/RMJ-12-2015-0042>
- [5] John, Huetter. *Blockchain Technology. Automotive recycling*, 2018, 38(3):30-37.
- [6] Sikorski J J , Haughton J , Kraft M . Blockchain technology in the chemical industry: Machine-to-machine electricity market. *Applied Energy*, 2017, 195(JUN.1):234-246. <https://doi.org/10.1016/j.apenergy.2017.03.039>
- [7] Zhang Y , Wen J . The IoT electric business model: Using blockchain technology for the internet of things. *Peer-to-Peer Networking and Applications*, 2017, 10(4):983-994. <https://doi.org/10.1007/s12083-016-0456-1>
- [8] Miraz M H , Ali M . Applications of Blockchain Technology beyond Cryptocurrency. *Annals of Emerging Technologies in Computing*, 2018, 2(1):1-6. <https://doi.org/10.33166/AETiC.2018.01.001>
- [9] Wang J , Peng W U , Wang X , et al. The outlook of blockchain technology for construction engineering management. *Frontiers of Engineering Management*, 2017, 4(01):71-79. <https://doi.org/10.15302/J-FEM-2017006>
- [10] Eyal, Ittay. *Blockchain Technology: Transforming Libertarian Cryptocurrency Dreams to Finance and Banking Realities*. *Computer*, 2017, 50(9):38-49. <https://doi.org/10.1109/MC.2017.3571042>
- [11] Study on the application of fly ash to the replacement of full strength cement in paste filling . *Shandong coal science and technology*, 2017,000(011):173-174
- [12] Chen Jie, Liu Yong, Shi Ying, et al. Study on gangue combination fly ash paste filling material . *Materials science and technology*, 2016,024(003):80-84
- [13] Maybury J , Ho J C M . Shear thickening of cement powder paste – why and how to mitigate?. *Transactions Hong Kong Institution of Engineers*, 2017, 24(4):193-203. <https://doi.org/10.1080/1023697X.2017.1375433>
- [14] Xie H P , Gao F , Ju Y , et al. Quantitative definition and investigation of deep mining. *Mtan Xuebao/Journal of the China Coal Society*, 2015, 40(1):1-10.
- [15] Kumari S , Li X , Wu F , et al. Design of a provably secure biometrics-based multi-cloud-server authentication scheme. *Future Generation Computer Systems*, 2017, 68(mar.):320-330. <https://doi.org/10.1016/j.future.2016.10.004>
- [16] Anglano C , Canonico M , Guazzone M . FC2Q: exploiting fuzzy control in server consolidation for cloud applications with SLA constraints. *Concurrency & Computation Practice & Experience*, 2015, 27(17):4491-4514. <https://doi.org/10.1002/cpe.3410>
- [17] Rashmi, Chawla V , Sehgal R , et al. The RC7 Encryption Algorithm. *International Journal of Security and its Applications*, 2015, 9(5):55-60. <https://doi.org/10.14257/ijssia.2015.9.5.05>

- [18] Zhang X , Wang X . *Multiple-image encryption algorithm based on mixed image element and permutation. Computers & Electrical Engineering*, 2017, 62(MAY):6-16. <https://doi.org/10.1016/j.optlaseng.2016.12.005>
- [19] Singh S , Attri V K . *Dual Layer Security of data using LSB Image Steganography Method and AES Encryption Algorithm. International Journal of Signal Processing Image Processing & Pattern Recognition*, 2015, 8(5):259-266. <https://doi.org/10.14257/ijcip.2015.8.5.27>
- [20] Liu L , Hao S , Lin J , et al. *Image block encryption algorithm based on chaotic maps. IET Signal Processing*, 2018, 12(1):22-30. <https://doi.org/10.1049/iet-spr.2016.0584>
- [21] Ma Z , Jiang M , Gao H , et al. *Blockchain for digital rights management. Future Generation Computer Systems*, 2018, 89(DEC.):746-764. <https://doi.org/10.1016/j.future.2018.07.029>
- [22] Xie F , Chen H . *An Efficient and Robust Data Integrity Verification Algorithm Based on Context Sensitive. International Journal of Security and its Applications*, 2016, 10(4):33-40. <https://doi.org/10.14257/ijisia.2016.10.4.04>
- [23] Kumar M , Chand S , Katti C P . *A Secure End-to-End Verifiable Internet-Voting System Using Identity-Based Blind Signature. IEEE Systems Journal*, 2020, 14(2):2032-2041. <https://doi.org/10.1109/JSYST.2019.2940474>
- [24] Wang X , Lin Y , Yao G . *Data integrity verification scheme with designated verifiers for dynamic outsourced databases. Security & Communication Networks*, 2015, 7(12):2293-2301. <https://doi.org/10.1002/sec.938>
- [25] Lin C , Shen Z , Chen Q , et al. *A data integrity verification scheme in mobile cloud computing. Journal of Network and Computer Applications*, 2017, 77(jan.):146-151. <https://doi.org/10.1016/j.jnca.2016.08.017>
- [26] Shan, P., Lai, X., & Liu, X. (2019) "Correlational Analytical Characterization of Energy Dissipation-Liberation and Acoustic Emission during Coal and Rock Fracture Inducing by Underground Coal Excavation", *Energies*, 12(12), pp. 2382. <https://doi.org/10.3390/en12122382>.
- [27] Shan, P., & Lai, X. (2019) "Mesoscopic structure PFC similar to 2D model of soil rock mixture based on digital image", *Journal of Visual Communication and Image Representation*, 58, pp. 407-415. <https://doi.org/10.1016/j.jvcir.2018.12.015>
- [28] Tang, Y.; Feng, W.\*; Chen, Z.\*; Nong, Y.; Guan, S.; Sun, J. *Fracture behavior of a sustainable material: Recycled concrete with waste crumb rubber subjected to elevated temperatures. Journal of Cleaner Production* 2021, 318: 128553. <https://doi.org/10.1016/j.jclepro.2021.128553>
- [29] Zhao, Y., Bai, C., Xu, C., & Foong L. K. (2021). *Efficient metaheuristic-retrofitted techniques for concrete slump simulation. Smart Structures and Systems*, 27 (5), 745-759.